J|A|C|S
ARTICLES
Published on Web 07/13/2002

Quantum Control of Molecular Chirality: Optical Isomerization of Difluorobenzo[*c*]phenanthrene

Hiroaki Umeda,[†] Masato Takagi,[‡] Saburou Yamada,[‡] Shiro Koseki,*[,†] and Yuichi Fujimura*[,§]

Contribution from the Department of Material Science, College of Integrated Arts and Sciences, Osaka Prefecture University, 1-1 Gakuen-cho, Sakai, Osaka 599-8531, Japan, Chemistry Department for Materials, Faculty of Engineering, Mie University, 1515 Kamihama, Tsu 514-8507, Japan, and Department of Chemistry, Graduate School of Science, Tohoku University, Sendai 980-8578, Japan

Received December 21, 2001

Abstract: The results of a theoretical study are presented on quantum control of a chiral exchange reaction of a polyatomic molecule by using infrared laser pulses. Difluorobenzo[*c*]phenanthrene was chosen to be the simplest model for its helical chirality exchange reaction. This molecule has two stable configurations: *M* and *P* forms. From the viewpoint of chemical reaction dynamics, isomerization is regarded as the movement of one of the two representative points that initially correspond to the two forms to the position of the other representative point, while the other representative point remains in its initial position. The ground-state potential energy surface and dipole moment functions required to control this reaction were evaluated at the MP2/6-31+G(d,p) and MP2/TZV+(d,p) levels of molecular orbital (MO) theory. An effective potential energy surface (PES) that is a function of twisting motion of the benzene rings and wagging motion of the CF_2 group was constructed on the basis of the MO results. An analytical expression for the effective PES and that for the dipole moment functions were prepared to make the isomerization control tractable. A quantum control method in a classical way was applied to the isomerization of preoriented difluorobenzo[*c*]phenanthrene in low temperature limits. The time evolution of the representative point of the *M* form and that of the *P* form are separately evaluated to determine the optimal laser fields. This means that the laser control produces pure helical enantiomers from a racemic mixture. Representative points are replaced by the corresponding nuclear wave packets in this treatment. The derived control laser field consists of two linearly polarized E_x and E_z components that are perpendicular to each other. These components are π-phase-shifted when the representative point is in the transition-state regions. Under the irradiation of this laser pulse, one of the two representative points of the isomerization is transferred to the target position along the intrinsic reaction path between the enantiomers, while the other representative point remains in its initial potential well. This results in one-way isomerization control, that is, the *M*(*P*) to *P*(*M*) form. The isomerization is completed with yields of ca. 70% within a few picoseconds. Temporal behaviors of the nuclear wave packet whose center corresponds to the representative point are drawn to see how the desired chiral exchange reaction proceeds in the presence of the control field, while its reverse process is suppressed.

1. Introduction

Molecular chirality is one of the fundamental characteristics of molecules,[1] and it plays an important role in stereochemistry and biochemistry.[2−4] For practical purposes, pure enantiomers with chirality, that is, *M* and *P* forms, are synthesized by the use of a specific catalysis to its chiral precursor.[2]

In recent years, with the development of laser technology, attractive attention has been paid to quantum control of molecular chirality because the use of the coherent nature of lasers is expected to create a new control scenario.[3] It is well known that chiral molecules are produced by photoreactions of racemic mixtures by irradiating a right or left circularly polarized laser.[4] However, the resultant yield of enantiomer excess is very low,[5] and a sophisticated laser pulse is needed to create a sufficient yield of enantiomer excess.[6] Shapiro and Brumer[7]

* To whom correspondence should be addressed. E-mail: S.K., shiro@ms.cias.osakafu-u.ac.jp; Y.F., fujimura@mcl.chem.tohoku.ac.jp.
[†] Osaka Prefecture University.
[‡] Mie University.
[§] Tohoku University.

(1) Avalos, M.; Babiano, R.; Cintas, P.; Jimenez, J.; Palacios, J. C.; Barron, L. D. *Chem. Rev.* **1998**, *98*, 2391.
(2) Noyori, R. *Asymmetric Catalysis in Organic Synthesis*; Wiley: New York, 1994.
(3) Hoki, K.; Fujimura, Y. In *Laser Control and Manipulation of Molecules*; Bandrauk, A. D., Fujimura, Y., Gordon, R. J., Eds.; ACS Symposium Series 821; American Chemical Society: Washington, DC, 2002; p 32.
(4) Inoue, Y. *Chem. Rev.* **1992**, *92*, 741.
(5) Shao, J.; Hänggi, P. *J. Chem. Phys.* **1997**, *107*, 9935.
(6) Salam, A.; Meath, W. J. *J. Chem. Phys.* **1997**, *106*, 7865; *Chem. Phys.* **1998**, *228*, 115.
(7) Shapiro, M.; Brumer, P. *J. Chem. Phys.* **1991**, *95*, 8658.

10.1021/ja017849f CCC: $22.00

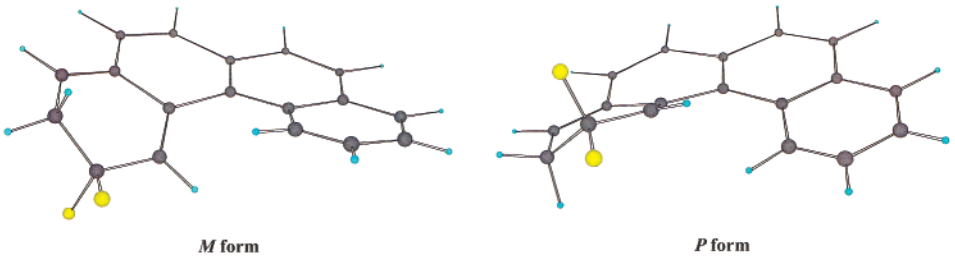

Figure 1. Enantiomers (*M* and *P* forms) of difluorobenzo[*c*]phenanthrene.

proposed a method for coherent control of an enantiomer-selective preparation in a model system using achiral lasers, that is, linearly polarized lasers. Cina and Harris[8] developed a wave packet theory for the preparation and phase control of superposition states of two enantiomers created in an electronically excited state from a double-well model potential in the ground state.

Chiral molecules are classified into three groups depending on their chiralities, that is, axial, helical, and point chiralities. In this paper, we present the results of a theoretical study on the quantum control of difluorobenzo[*c*]phenanthrene possessing helical chirality as shown in Figure 1. This investigation is the first step toward the establishment of a method for controlling the isomerization reaction between *M* and *P* forms of DNA.

Most previous studies on quantum control of optical isomerization reactions have treated molecules possessing axial chirality mainly on the basis of a one-dimensional symmetric double-well potential model, as proposed by Hund just after the establishment of modern quantum mechanics.[9] Selective preparation of pure enantiomers was modeled as an exchange between two enantiomers via a quantum tunneling through a one-dimensional double-well potential in the ground state or via an achiral electronic excited state.[10−19] An example of the former is H_2POSH, which has axial chirality.[10] The S−H torsion around the P−S bond was used as a one-dimensional reaction coordinate in that study. In subsequent studies, selective preparation of pure enantiomers was achieved from a racemic mixture of H_2POSH via the lowest electronic excited state.[18,19] Gerbasi et al.[20] recently proposed a theory of enantiomeric control in 1,3-dimethylallene with axial chirality using achiral pulses. In their study, the reaction coordinate is the dihedral angle between the $H_3C-C{=}C$ and $C{=}C-CH_3$ planes. The C−C−C bending mode is also taken into account. They treated a population change in both the total angular momentum and the *z*-component selected state of 1,3-dimethylallene.

There are two fundamental issues regarding the treatment of polyatomic molecules possessing helical chirality in comparison with those possessing axial chirality. The first issue is related to reaction coordinates. Generally, the most probable reaction path cannot be described in terms of a one-dimensional symmetric or asymmetric double-well potential curve, because a symmetric structure is not always a true transition state for isomerization reactions. An asymmetric transition-state structure should be described by more than one vibrational degree of freedom along isomerization paths. Thus, it is essential to take multidimensional reaction coordinates into account.

The second issue is related to the mechanism of chiral exchange reactions. The tunneling mechanism works well for reactions with light atoms on its double-well potential. However, such reactions in a large molecule possessing helical chirality are practically forbidden in usual thermal conditions without any catalysis. Furthermore, there are two representative points in chiral exchange reactions: one corresponds to the *M* form of difluorobenzo[*c*]phenanthrene, and the other corresponds to the *P* form. Therefore, we have to treat these two representative points that move on its reaction potential energy surface (PES). These two subjects are taken into account in the present paper.

In the next section, an effective model PES and dipole moment surface are constructed for isomerization between two enantiomers of difluorobenzo[*c*]phenanthrene (*M* and *P* forms in Figure 1). Two fluorine atoms are introduced for the dipole moment to be changed drastically along the reaction path. All molecular orbital (MO) calculations were performed using the GAMESS suite of program codes.[21] An analytical model of a two-dimensional PES and dipole moment functions is proposed on the basis of the MO results on the isomerization reaction. In section 3, a quantum control theory in a classical way is applied to this reaction to design appropriate control laser fields.[22] Two representative points corresponding to the *M* and *P* forms are separately obtained by solving the time-dependent Schrödinger equation. This is a simplified treatment of quantum control of the optical isomerization in a racemic mixture.

2. An Ab Initio Molecular Orbital Study

2.a. Model Potential Energy Surface (PES): Reaction Coordinates. The equilibrium and transition-state structures were optimized using the RHF/6-31G+(d,p) method,[23−25] in

(8) Cina, J. A.; Harris, R. A. *J. Chem. Phys.* **1994**, *100*, 2531; *Science* **1995**, *267*, 832.
(9) Hund, F. *Z. Phys.* **1927**, *43*, 8050.
(10) Fujimura, Y.; González, L.; Hoki, K.; Manz, J.; Ohtsuki, Y. *Chem. Phys. Lett.* **1999**, *306*, 1; *Chem. Phys. Lett.* **1999**, *310*, 578.
(11) Shapiro, M; Frishman, E.; Brumer, P. *Phys. Rev. Lett.* **2000**, *84*, 1669.
(12) Fujimura, Y.; González, L.; Hoki, K.; Kröner, D.; Manz, J.; Ohtsuki, Y. *Angew. Chem., Int. Ed.* **2000**, *39*, 4586; *Angew. Chem.* **2000**, *112*, 4785.
(13) González, L.; Hoki, K.; Kröner, D.; Leal, A.; Manz, J.; Ohtsuki, Y. *J. Chem. Phys.* **2000**, *113*, 11134.
(14) Fujimura, Y.; González, L.; Hoki, K.; Manz, J.; Ohtsuki, Y.; Umeda, H. *Advances in Multiphoton Processes and Spectroscopy*; World Scientific: Singapore, 2001; Vol. 14, p 30.
(15) Hoki, K.; Ohtsuki, Y.; Fujimura, Y. *J. Chem. Phys.* **2001**, *114*, 1575.
(16) Leal, A.; Kröner, D.; González, L. *Eur. J. Phys. D* **2001**, *14*, 185.
(17) Doslic, N.; Fujimura, Y.; González, L.; Hoki, K.; Kröner, D.; Kühn, O.; Manz, J.; Ohtsuki, Y. In *Femtochemistry*; de Schryver, F. C., de Feyter, S., Schweitzer, G., Eds.; Wiley-VCH: Weinheim, 2001; p 189.
(18) González, L.; Kröner, D.; Solá, I. R. *J. Chem. Phys.* **2001**, *115*, 2519.
(19) Hoki, K.; González, L.; Fujimura, Y. *J. Chem. Phys.* **2002**, *116*, 2433.
(20) Gerbasi, D.; Shapiro, M.; Brumer, P. *J. Chem. Phys.* **2001**, *115*, 5349.
(21) Schmidt, M. W.; Baldridge, K. K.; Boatz, J. A.; Elbert, S. T.; Gordon, M. S.; Jensen, J. H.; Koseki, S.; Matsunaga, N.; Nguyen, K. A.; Su, S.; Windus, T. L.; Dupuis, M.; Montgomery, J. A., Jr. *J. Comput. Chem.* **1993**, *14*, 1347.
(22) Umeda, H.; Fujimura, Y. *J. Chem. Phys.* **2000**, *113*, 3510; *Chem. Phys.* **2001**, *274*, 231.
(23) Ditchfield, R.; Hehre, W. J.; Pople, J. A. *J. Chem. Phys.* **1971**, *54*, 724.
(24) Hehre, W. J.; Ditchfield, R.; Pople, J. A. *J. Chem. Phys.* **1972**, *56*, 2257.
(25) Francl, M. M.; Pietro, W. J.; Hehre, W. J.; Binkley, J. S.; Gordon, M. S.; DeFrees, D. J.; Pople, J. A. *J. Chem. Phys.* **1982**, *77*, 3654.

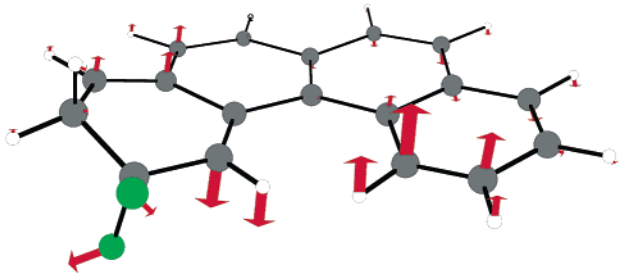

Figure 2. Geometrical structure of the transition state (**TS**). Because this is also an enantiomer, the mirrored structure exists. Arrows indicate the reaction mode possessing an imaginary frequency at **TS**. The corresponding vibrational motion consists essentially of Q_2 at this geometry and leads to the energy minimum (**EQ**), that is, the *M* form, and where the reverse motion derives the strong interaction between Q_1 and Q_2 and finally reaches the other energy minimum (the *P* form). The former motion corresponds to the IRC of 0 through 12 [amu$^{1/2}$ bohr] in Figure 3, while the strong mixture of Q_1 and Q_2 in the latter occurs in the flat area of the potential energy near the IRC of −10 [amu$^{1/2}$ bohr].

Table 1. Relative Energies [kcal/mol] of Stationary Structures

	RHF/ 6-31+G(d,p)	MP2/ 6-31+G(d,p)	RHF/ TZV+(d,p)	MP2/ TZV+(d,p)
EQ	0	0	0	0
TS	6.7	7.6	6.3	8.0
TS2	8.5	10.6	8.0	11.5

which diffuse sp functions were added only to fluorine atoms.[26] The optimized geometry of the equilibrium (**EQ**) has a nonplanar carbon skeleton as illustrated in Figure 1.

When the geometrical structure is assumed to have C_s symmetry (the carbon skeleton being planar), the RHF optimized geometry is found to have two imaginary frequencies of vibrational motions; the C_s structure is a second-order transition state (**TS2**). One of the motions is a twisting motion of benzene rings (194*i* cm^{-1}), and the other is a wagging motion of the CF_2 group (62*i* cm^{-1}). In our further investigation, the true transition state (**TS**) of this isomerization was successfully located as shown in Figure 2. The arrows in Figure 2 indicate the reaction mode in which the vibrational frequency is 149*i* cm^{-1}.

The relative energies of these stationary structures are calculated to be 0 (**EQ**), 6.7 (**TS**), and 8.5 (**TS2**) kcal/mol at the RHF/6-31+G(d,p) level of theory (see Table 1). A more extended basis set, TZV+(d,p), gave results similar to those of 6-31+G(d,p). Accordingly, the 6-31+G(d,p) basis set was used in the following investigation because of appropriate computational time.

To construct a PES along this isomerization, the intrinsic reaction coordinate (IRC) or minimum energy path between enantiomers was generated using the second-order Gonzales−Schlegel method[27] at the RHF/6-31+G(d,p) level of MO theory. It is apparent that the twisting motion of two benzene rings is essential in the early stage along the IRCs starting at **TS** forward and backward along the reaction coordinate. One of the IRCs, referred to as IRC-f (where f means forward), reaches straightforward to **EQ**, but IRC-b (where b means backward) gets through to a very flat area of the PES (Figure 3a). The total energy of the system still decreases gradually along IRC-b, and no stationary point is found in this flat area. After passing this

(26) The diffuse sp exponent is 0.1076 for fluorine atoms.
(27) Gonzales, C.; Schlegel, H. B. *J. Chem. Phys.* **1989**, *90*, 2154.

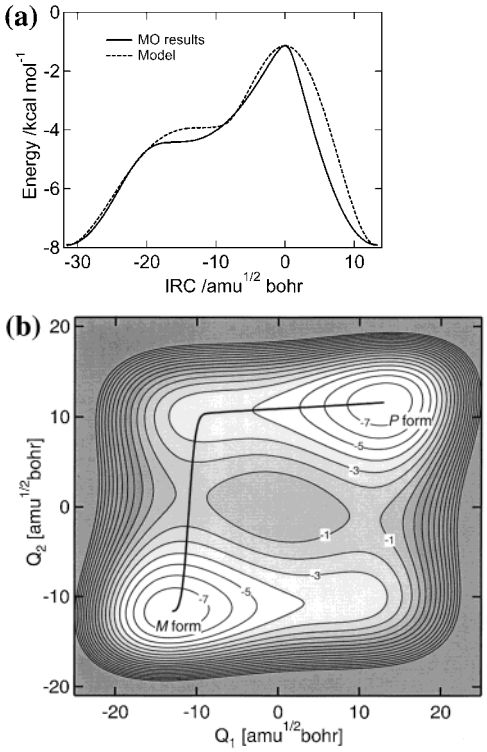

Figure 3. (a) Potential energy curves along the intrinsic reaction coordinate (IRC) connecting the enantiomers. The curve drawn by a solid line is obtained by using the MO method (RHF/6-31+G(d,p)), and that drawn by a dashed line is generated by the model potential energy function $V(Q_1,Q_2)$. Q_1 varies principally in the IRC range of [−30, −10], while Q_2 varies in the IRC range of [−10, 10]. The *M* form is located near the IRC of 10 [amu$^{1/2}$ bohr], and the *P* form is near the IRC of −30 [amu$^{1/2}$ bohr]. (b) Contour map [kcal/mol] of the potential energy surface $V(Q_1,Q_2)$ for isomerization. Q_1 and Q_2 are the wagging motion of the CF_2 group and the twisting motion of the benzene rings, respectively. The solid line indicates the IRC shown in Figure 3a. The energy minima are located at (Q_1,Q_2) = (−13.0, −11.6) and (13.0, 11.6) corresponding to the *M* and *P* forms, respectively, while **TS**'s are at (Q_1,Q_2) = (−10.8, 1.3) and (10.8, −1.3).

area, the principal motion of the reaction is changed to wagging motion of the CF_2 group, and, finally, the system reaches **EQ**.

Thus, the results of IRC analysis show that wagging motion Q_1 of the CF_2 group and twisting motion Q_2 of the benzene rings are principal modes in this optical isomerization reaction, and the other 88 motions can be considered as not being essential for the isomerization. Therefore, we decided to employ a two-dimensional PES in the following dynamical study to design control laser fields. Because **TS2** has a planar structure, and the separate Q_1 and Q_2 motions lead to a double well, and because **TS** is also an enantiomer, it can be assumed that the two-dimensional PES is expressed by a fourth-order polynomial of reaction coordinates Q_1 and Q_2 as

$$V(Q_1,Q_2) = aQ_1^4 + bQ_2^4 + cQ_1^2 + dQ_2^2 + eQ_1Q_2 \qquad (1)$$

where the parameters $a = 0.8237 \times 10^{-4}$, $b = 0.3062 \times 10^{-3}$, $c = -0.2032 \times 10^{-1}$, $d = -0.7326 \times 10^{-1}$, and $e = -0.1676 \times 10^{-1}$ were determined to reproduce the PES along the IRC connecting **EQ**, **TS**, and **TS2**, where *a* and *b* are in amu^{-2} bohr^{-4} kcal/mol, and *c*, *d*, and *e* are in amu^{-1} bohr^{-2} kcal/mol. As shown in Figure 3a, even though the details are somewhat different, the overall shape of PES along the IRC is the same as that obtained using the RHF/6-31+G(d,p) method. Figure 3b shows a contour map of the PES $V(Q_1,Q_2)$. The energy

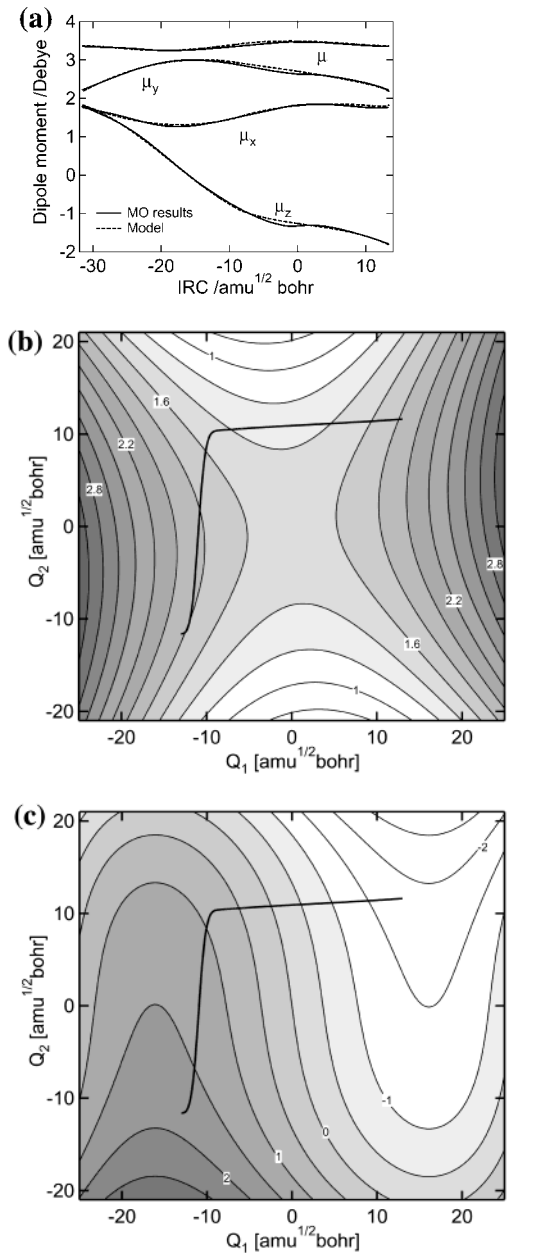

Figure 4. (a) Dipole moment [debye] and their components along the intrinsic reaction coordinate (IRC). The curve drawn by a solid line is obtained by the MO calculation, and that drawn by a dashed line is generated by the model function $\mu(Q_1,Q_2)$ in eq 2. (b) Contour map of the dipole moments $\mu_x(Q_1,Q_2)$ in debye. The solid line indicates the IRC. (c) Contour map of the dipole moments $\mu_z(Q_1,Q_2)$ in debye. The solid line indicates the IRC.

minima are located at $(Q_1,Q_2) = (-13.0, -11.6)$ and (13.0, 11.6) corresponding to the *M* and *P* forms, respectively, while **TS**'s are at $(Q_1,Q_2) = (-10.8, 1.3)$ and $(10.8, -1.3)$.

2.b. Dipole Moment Functions. It is essential to know reaction-coordinate dependence of the dipole moments along the isomerization to design a control laser pulse. The dipole moment and its components along the IRC are obtained as shown in Figure 4a. Only the *z* component is changed drastically along the IRC (see Scheme 1). Although both *x* and *y* components are not greatly changed, the *x* component, as well as the *z* component, is chosen to control the isomerization reaction.

Scheme 1

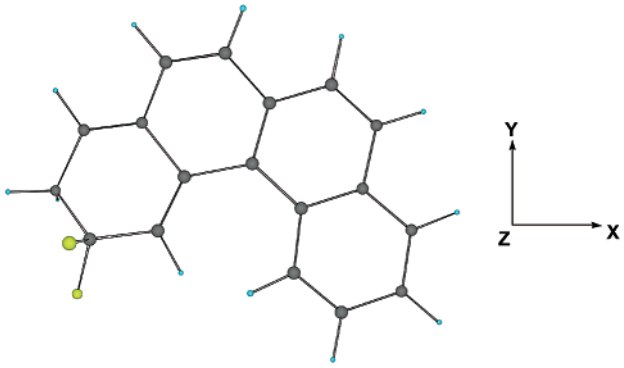

It is assumed that two-dimensional functions $\mu(Q_1,Q_2)$ of dipole moments can be expressed as

$$\mu_x(Q_1,Q_2) = \alpha_x Q_1^2 + \beta_x Q_2^2 + \gamma_x Q_1 Q_2 + \delta_x \qquad (2a)$$

$$\mu_y(Q_1,Q_2) = \alpha_y Q_1^2 + \beta_y Q_2^2 + \gamma_y Q_1 Q_2 + \delta_y \qquad (2b)$$

$$\mu_z(Q_1,Q_2) = \alpha_z Q_1^3 + \beta_z Q_2^3 + \gamma_z Q_1 + \delta_z Q_2 \qquad (2c)$$

where the parameters α, β, γ, and δ have been determined to reproduce both of the dipole moments along the IRC as shown in Figure 4a.

$\alpha_x = 0.25 \times 10^{-2}$ $\beta_x = -0.18 \times 10^{-2}$ $\gamma_x = 0.80 \times 10^{-3}$ $\delta_x = 1.53$
$\alpha_y = -0.26 \times 10^{-2}$ $\beta_y = -0.23 \times 10^{-2}$ $\gamma_y = -0.22 \times 10^{-3}$ $\delta_y = 2.98$
$\alpha_z = 0.18 \times 10^{-3}$ $\beta_z = -0.10 \times 10^{-3}$ $\gamma_z = -0.14$ $\delta_z = -0.20 \times 10^{-1}$

where α_x, β_x, γ_x, α_y, β_y, and γ_y are in amu^{-1} bohr^{-2} debye, and δ_x and δ_y are in debye. The constants α_z and β_z are in amu$^{-3/2}$ bohr^{-3} debye, and γ_z and δ_z are in amu$^{-1/2}$ bohr^{-1} debye. The dipole moment surfaces determined for the *x* and *z* components are shown in Figure 4b and c, respectively. In this figure, the IRC path is also shown as a solid line.

3. Quantum Control of Isomerization of Difluorobenzeno[*c*]phenanthrene

The theoretical treatment for obtaining control pulses is based on quantum control in a classical way that was reviewed elsewhere.[22] In that treatment, the dynamical behavior is described in terms of a representative point moving on the PES as in the classical treatment of chemical reaction dynamics. To manipulate the representative point to the target position, impulsive laser pulses change the magnitudes of its linear momentum. That is, these are increased for the representative point to climb up the reaction barrier, and after crossing over the barrier, they are decreased for the representative point to reach the target position. In the quantum control theory, the expression for the control field is derived from classical mechanics, and a representative point is replaced by the corresponding nuclear wave packet. The temporal evolution of the wave packet is determined by solving the time-dependent Schrödinger equation of the reaction system, and the position and linear momentum of the representative point involved in the expression for the control field are replaced by the quantum-mechanical expectation value.

The amplitude of the control pulse is given as

$$E(t) = -f(Q)\left(\frac{\partial \mu}{\partial Q}\right)\langle P(t)\rangle \tag{3}$$

where $Q \equiv \langle Q(t)\rangle$, $f(Q)$ is a parameter controlling the kinetic energy of the representative point,[22] and $(\partial\mu/\partial Q)$ is the dipole derivative with respect to the reaction coordinate Q. A quantum-mechanically averaged position and a linear momentum of the representative point are expressed as $\langle Q(t)\rangle = \langle \Psi(t)|Q|\Psi(t)\rangle$ and $\langle P(t)\rangle = \langle \Psi(t)|P|\Psi(t)\rangle$, respectively. Here, the nuclear wave packet $\Psi(t)$ satisfies the time-dependent Schrödinger equation in the semiclassical treatment of the laser field−molecule interaction

$$i\hbar\frac{\partial}{\partial t}\Psi(t) = \hat{H}(Q_1,Q_2,t)\Psi(t) \tag{4}$$

The semiclassical Hamiltonian in the dipole approximation $\hat{H}(Q_1,Q_2,t)$ is expressed as

$$\hat{H}(Q_1,Q_2,t) = \hat{T}(Q_1) + \hat{T}(Q_2) + V(Q_1,Q_2) - \mu(Q_1,Q_2)\cdot E(t) \tag{5}$$

where $\hat{T}(Q_1)$ ($\hat{T}(Q_2)$) denotes the kinetic energy operator of the vibrational mode Q_1 (Q_2).

The control field is designed for the representative point to accelerate the linear momentum for it to climb up the reaction barrier and to decelerate the linear momentum for it to reach the target position by adjusting the parameter $f(Q)$. The actual computation procedure consists of iterative substitution of $E(t)$ into the time-dependent Schrödinger equation to obtain the nuclear wave function by which a new $E(t)$ is evaluated at an advanced time.

Difluorobenzo[*c*]phenanthrene is assumed to be preoriented at a space-fixed position as shown in Scheme 1. An optical isomerization of preoriented difluorobenzo[*c*]phenanthrene from the *M* to *P* form will be controlled by two linearly (*x*- and *z*-) polarized IR pulses, $E_x(t)$ and $E_z(t)$ in the following study. The *M* and *P* forms are expressed in terms of two corresponding representative points, respectively.

To control two representative points at the same time in the molecular chiral exchange reaction, we adopted a simplified treatment based on the time-dependent Schrödinger equation. In this simplified treatment, first, we individually evaluated the field $E^{(M)}(t)$ and $E^{(P)}(t)$, which are constructed from information on the wave packets of the *M* and *P* forms, respectively. That is, the time-dependent Schrödinger equations are solved for the *M* and *P* forms separately. This means that this simplified treatment is a quantum control of molecular chirality in a racemic mixture. An explicit treatment of optical isomerization in a racemic mixture should be carried out using the Liouville equation of the density matrix.[3,12,15,19] We then averaged these fields to obtain the control field, that is, $E(t) = aE^{(M)}(t) + bE^{(P)}(t)$, where *a* and *b* are constants. To manipulate the *M* form of the representative point in such a way that it crosses over the potential barrier to reach the target while the other representative point remains in its initial potential well, we set $f(Q)$ for the *M* form wave packet along the Q_1 coordinate as

$$f^{(M)}_{Q_1}(Q_1,Q_2) = 1 \tag{6a}$$

and that along Q_2 as

$$f^{(M)}_{Q_2}(Q_1,Q_2) = \frac{3}{\pi}\tan^{-1}(Q_2 - 2) + 0.5 \tag{6b}$$

These expressions mean that the linear momentum of the representative point along Q_1 is always decelerated, while that of Q_2 is accelerated before crossing over the potential barrier. On the other hand, $f^{(P)}_{Q_1}(Q_1,Q_2) = f^{(P)}_{Q_2}(Q_1,Q_2) = 1$ were assumed for the *P* form wave packet, which prevents the representative point from moving away from the initial position. The constants *a* and *b* in the control field should be satisfied with the condition $a > b$ for an optical isomerization from the *M* to *P* form of difluorobenzo[*c*]phenanthrene in a racemic mixture.[3,15] The reaction yield is robust with respect to the ratio of these constants. In the present calculation, they were tentatively set to be $a/b = 4.7$ for isomerization to be completed within a restricted time $t_f = 10$ ps.

Figure 5a and b shows the temporal behaviors of the isomerization in the presence of the control field. The red and blue lines are the mean trajectories of the *M* and *P* forms, respectively. We can see that the representative point initially representing the *M* form moves to the target region of the *P* form after crossing over the reaction barrier along the IRC, while that of the *P* form remains in the original potential well. To visualize the dynamics of the isomerization process, the nuclear wave packet $|\Psi(t)|^2$ at 0, 4.5, and 4.9 ps is depicted by contours in Figure 5a, and that at $t = 10$ ps is depicted in Figure 5b. The wave packet of the *M* form $|\Psi^{(M)}(t)|^2$ at $t = 4.5$ ps, that is, just after crossing over the reaction barrier, still retains a well-localized structure with slight delocalization. The delocalized part is because of a reflection by the barrier near the transition state. The delocalization of the wave packet at 4.9 ps is because of the fact that the packet passes the flat area along the IRC. The wave packet at 10 ps is also delocalized widely in the potential well of the *P* form. This indicates that hot enantiomers of the *P* form are created. Wave packets originally representing the enantiomer of the *P* form $|\Psi^{(P)}(t)|^2$ are delocalized within its original potential well even in the presence of the control pulses. The isomerization from the *M* to *P* form is completed with the yield of ca. 70% within 3−4 ps, and the inverse process is suppressed by the control-field condition. Some differences are observed in positions between the mean trajectories and the centers of density of the corresponding wave packets, for example, at $t = 4.9$ and 10 ps. These differences originate from the spreads of the nuclear wave packets; especially a nonreactive component remains in the potential well of the *M* form.

Figure 6 shows the amplitudes of laser fields E_x and E_z designed by the control method. This figure indicates that they are π-phase-shifted from the initial time to around 4.5 ps, while they are not phase-shifted after 4.5 ps. These phase behaviors are essential in controlling isomerization reactions such as molecular chiral reactions by using linearly polarized laser fields. This can be explained by taking into account the force induced by laser fields. The force induced by a laser field is given by $F = (\partial\mu/\partial Q)\cdot\boldsymbol{E}(t)$. Let us consider how the *M* form representative point moves in the Q_2 direction on the basis of classical mechanics. From the gradient direction of the dipole moment function μ_x in Figure 4b, a positive E_x moves the *M* form representative point in an upper left-hand direction on the reaction potential energy surface just before it passes over the

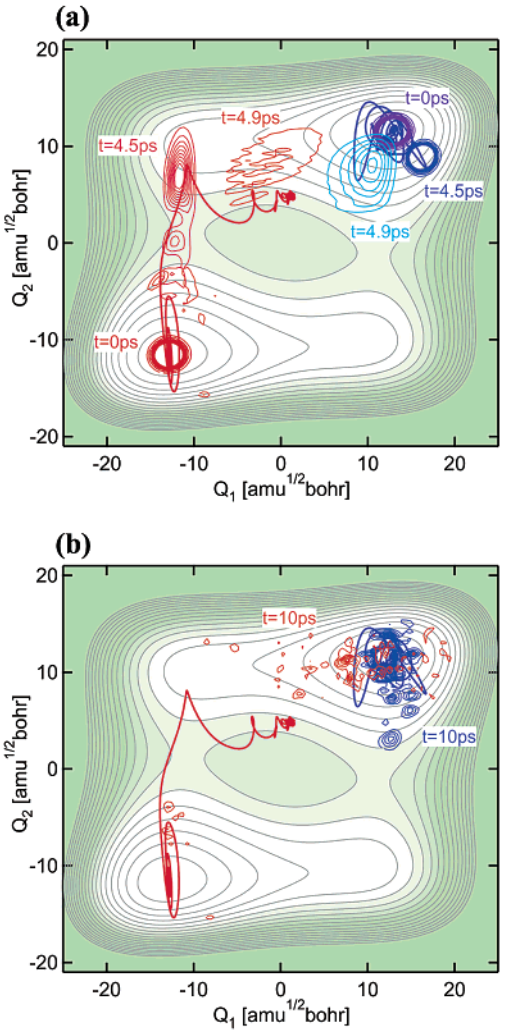

Figure 5. Wave packet dynamics of two representative points. The thick red and blue lines depict the mean trajectories of the *M* and *P* forms, respectively. The contours with the series of reddish colors show time evolution of the *M* form $|\Psi^{(M)}(t)|^2$, while those with the series of bluish colors show time evolution of the *P* form $|\Psi^{(P)}(t)|^2$. (a) $t = 0-4.9$ ps. (b) $t = 10$ ps (the end of the control period).

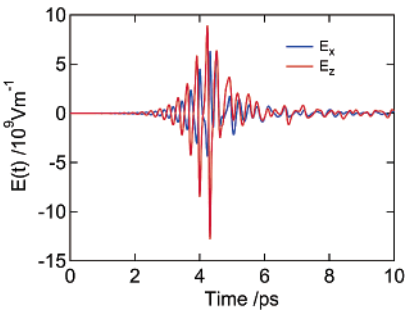

Figure 6. The designed control fields. E_x (blue) and E_z (red) denote the *x*- and *z*-polarized IR pulses, respectively. They are π-phase-shifted at $t = 0-4.5$ ps. After the representative point of the *M* form runs across the energy barrier, the phase of E_x is changed ($t > 4.5$ ps).

transition-state region. On the other hand, a positive E_z moves in a lower left-hand direction. As a result, a positive (negative) E_x and a negative (positive) E_z are required in the early stage of the reaction to move the *M* form representative point in the Q_2 direction, that is, π-phase-shifted field. After the representative point passes over the transition-state region, E_x again changes its phase of π, and this results in an in-phase between E_x and E_z. It should be also noted that the *P* form representative point does not move in the Q_2 direction under the above π-phase-shifted field condition. In this case, it seems that the *P* form representative point moves in the Q_1 direction at the same time, but because the central frequency of the field is different from that of the vibrational mode of Q_1, it cannot be activated effectively.

The designed pulses shown in Figure 6 are divided into three regions: 0−2, 2−6, and 6−10 ps. The pulses of the first and third regions are weak, and they are actually irrelevant to the optical isomerization control. The first region is because of our computational procedure in which a seeded pulse was used to produce the intense control pulses in the second time region. Therefore, the reaction control is completed within 3−4 ps. Such intense shaped pulses of $10^{12}-10^{13}$ W/cm^2 in the far IR frequency domain can be experimentally generated by using an amplified pulse-shaping apparatus combined with a difference frequency conversion.[28]

So far we have considered an optical isomerization from the *M* to *P* form in a racemic mixture. The reverse isomerization is controlled by the similar procedure, just by changing the relative phase between the linearly polarized pulses, $E_x(t)$ and $E_z(t)$, that is, keeping $E_z(t)$ but changing $E_x(t)$ to $-E_x(t)$, or vice versa. Thus, left/right polarizations of the laser pulses can be used to prepare the *M* or *P* form as well.

The present investigation employed a simplified model for difluorobenzo[*c*]phenanthrene of 90 vibrational degrees of freedom. In this model, we have taken into account only two vibrational modes that are directly associated with the helical chirality, and we omitted the other vibrational modes. Therefore, the effects because of mode couplings such as intramolecular vibrational-energy redistribution (IVR) were neglected. A theoretical treatment of IVR in quantum control of molecular chirality has been described elsewhere.[29]

4. Summary

We have presented the results of a theoretical study on reaction control of the isomerization of difluorobenzo[*c*]phenanthrene in a racemic mixture. This molecule is the simplest model possessing helical chirality. The intrinsic reaction coordinate was obtained using the RHF/6-31+G(d,p) method, and the relative energies were reexamined at higher levels of molecular orbital theory: MP2/TZV+(d,p). On the basis of the molecular orbital results, we decided that the isomerization reaction should be described by a model potential energy surface including only two vibrational motions: twisting motion of benzene rings and wagging motion of the CF_2 group. The *M* and *P* forms are expressed in terms of two corresponding representative points. By applying a quantum control method in a classical way to the isomerization between the *M* and *P* forms in a racemic mixture, we obtained the yield of ca. 70% within 10 ps. This method is a simplified approach to the laser conversion of a racemate to pure helical enantiomers because the time-dependent Schrödinger equations for *M* and *P* forms are separately solved. The control field consists of two linearly polarized IR pulses with the π-phase shifted in the early stage of the reaction. In

(28) Goswami, D.; Sandhu, A. S. *Advances in Multiphoton Processes and Spectroscopy*; World Scientific: Singapore, 2001; Vol. 14, p 132.
(29) Ohta, Y.; Hoki, K.; Fujimura, Y. *J. Chem. Phys.* **2002**, *116*, 7509.

that time, the representative point crosses over the potential barrier. The phase shift is the origin of the transfer of only one of the two representative points to the target position. The temporal behavior of the reaction dynamics was analyzed in terms of the nuclear wave packets corresponding to two representative points on the reaction potential surface.

Acknowledgment. We would like to thank Professor J. Manz for his critical comments. This work was supported by grants from the Science and Technology Agency of Japan (to H.U. and S.K.), by a German−Japanese International Joint Research Project, by a Grant-in-Aid for Scientific Research from The Ministry of Education, Culture, Sports, Science, and Technology of Japan (Nos. 10640480 and 13640497) (to Y.F.), and by a Grant-in-Aid for Scientific Research on Priority Areas (A) (No. 11166205). H.U. is a postdoctoral research fellow, Fuji Research Institute.

JA017849F